ChemComm

COMMUNICATION

View Article Online
View Journal | View Issue

Cite this: *Chem. Commun.*, 2025, **61**, 16380

Received 1st August 2025,
Accepted 14th September 2025

DOI: 10.1039/d5cc04405g

rsc.li/chemcomm

Enantioselective gold(I)-catalysed alkyne hydroarylations for inherently chiral calix[4]arenes

Mehri Goudarzi,[a] Anuruddha Alagiyawanna,[b] Andrea Serafino,[b] Silvia Rizzato,[c] Francesco Bertocchi,[b] Francesca Terenziani,[b] Stefano Santoro,[d] Wenling Qin,[e] Gianpiero Cera *[b] and Valentina Pirovano *[a]

We report enantioselective gold(I)-catalysed hydroarylation of alkynes to access inherently chiral calix[4]arenes. This method delivered a family of macrocycles, embedded with phenanthrene motifs, with good yields and enantioselectivities. Investigations of the photophysical and chiroptical properties revealed interesting fluorescence features, suggesting potential applications in materials science and devices.

Hydroarylation reactions represent a powerful tool to construct organic molecules with many applications in the field of organic chemistry.[1] In this context, gold catalysis has been established as a versatile method able to transform modular alkyne derivatives into useful building blocks or materials in the most atom- and step-economical manner.[2] In particular, enantioselective gold-catalysed hydroarylation of alkynes has been applied for the synthesis of chiral compounds characterised by non-trivial axial,[3] planar[4] or helical[5] stereogenic elements (Scheme 1a and b). Recently, the scientific community has witnessed an increased interest in developing asymmetric catalytic methods to synthesize inherently chiral compounds.[6] This type of chirality arises from the introduction of "a curvature in an ideal planar structure that is devoid of symmetry axes in its bidimensional representation".[7] Among such organic compounds, inherently chiral calix[4]arenes (ICCs) are now in high demand.[8] This is demonstrated by numerous enantioselective catalytic methods that have been developed recently for the construction of such macrocycles in an asymmetric manner.[9] ICCs find many applications in chemosensory, medicinal chemistry, or materials science.[10] Moreover, their unique features have been employed to build synthetic molecular receptors[11] and catalysts.[12] Based on precedent studies,[13] we now exploit enantioselective gold catalysis for the construction of inherent chirality. The functionalisation of **1** at its *meta* position,[8b] *via* gold-catalysed hydroarylation of alkynes,[13b] results in the desymmetrisation of the macrocycle, producing the targeted inherently chiral calix[4]arene **2** (Scheme 1c).

Calix[4]arenes are known to adopt several distinct conformations beyond the most common *cone* (*i.e.* partial *cone*, 1, 3-alternate and 1,2-alternate). The latter arise from the rotation of the phenolic rings around the methylene bridges. However, the well-defined *cone* conformation offers an ideal platform to develop enantioselective catalytic desymmetrisations.[9b–j]

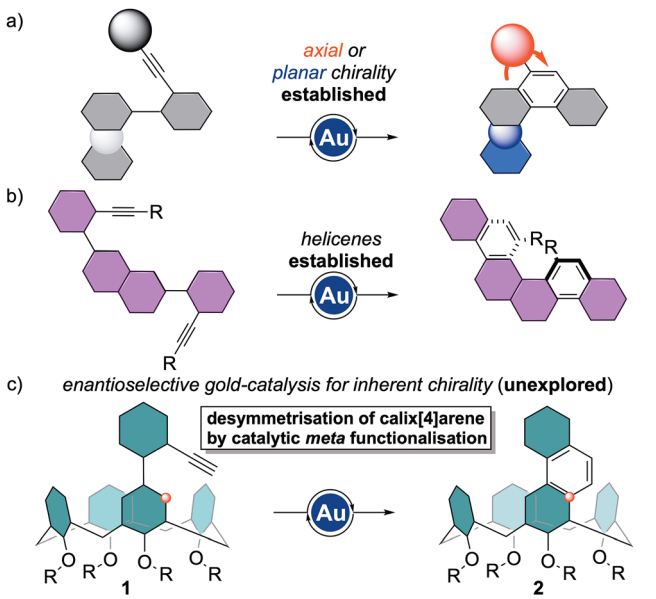

Scheme 1 "State-of-the-art" for enantioselective gold-catalysed hydroarylations of alkynes: (a) synthesis of axial, planar and (b) helical chiral compounds; (c) our work.

[a] *Dipartimento di Scienze Farmaceutiche, Sezione di Chimica Generale e Organica "A. Marchesini", Università degli Studi di Milano, Via G. Venezian 21, 20133, Milano, Italy. E-mail: valentina.pirovano@unimi.it*

[b] *Dipartimento di Scienze Chimiche, della Vita e della Sostenibilità Ambientale, Università di Parma, Parco Area delle Scienze 17/A, I-43124 Parma, Italy. E-mail: gianpiero.cera@unipr.it*

[c] *Dipartimento di Chimica, Università degli Studi di Milano, Via C. Golgi 19, 20133, Milano, Italy*

[d] *Dipartimento di Chimica, Biologia e Biotecnologie, Via Elce di Sotto, 8, 06123 Perugia, Italy*

[e] *Chongqing Key Laboratory of Natural Product Synthesis and Drug Research, School of Pharmaceutical Sciences, Chongqing University, Chongqing, 401331, P. R. China*

Table 1 Optimisation of the reaction conditions[a]

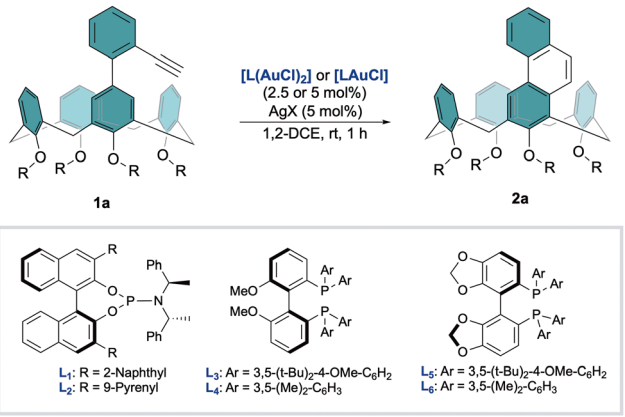

Entry	[Au]	AgX	2[b] (%)	e.r.[c]
1	[**L1**AuCl]	$AgNTf_2$	99	74 : 26
2	[**L2**AuCl]	$AgNTf_2$	89	57 : 43
3	[**L3**$(AuCl)_2$]	$AgNTf_2$	89	43 : 57
4	[**L4**$(AuCl)_2$]	$AgNTf_2$	87	72 : 28
5	[**L5**$(AuCl)_2$]	$AgNTf_2$	91	70 : 31
6	[**L6**$(AuCl)_2$]	$AgNTf_2$	91	86 : 14
7	[**L6**$(AuCl)_2$]	$AgSbF_6$	87	87 : 13
8	[**L6**$(AuCl)_2$]	$AgBF_4$	80	86 : 14
9	[**L6**$(AuCl)_2$]	AgOTf	87	86 : 14
10[d]	[**L6**$(AuCl)_2$]	$AgSbF_6$	65	48 : 52
11[e]	[**L6**$(AuCl)_2$]	SbF_6	99	90 : 10
12[ef]	[**L6**$(AuCl)_2$]	SbF_6	95	93 : 7

[a] Reaction conditions: **1a** (0.065 mmol), [Au] (2.5 or 5 mol%), $AgNTf_2$ (5 mol%) in anhydrous 1,2-DCE (0.65 ml, 0.1 M) at rt for 1 h. [b] Isolated yield. [c] Enantiomeric ratios (*e.r.*) were determined by chiral HPLC. See the SI for full experimental details. [d] Toluene (0.1 M) as the solvent. [e] CH_2Cl_2 (0.1 M) as the solvent. [f] Reaction performed at 0 °C for 18 hours.

Hence, it gives a rigid bowl-shaped geometry that helps the catalysts to discriminate the enantiotopic faces. In contrast, in non-*cone* conformations, the spatial arrangement is less defined, rendering asymmetric catalytic reactions more challenging. For this reason, we began our investigation with the synthesis of model calix[4]arene **1a**, "frozen" in a *cone* conformation.[14] The presence of bulky propyl groups at the lower-rim of the macrocycle is necessary to make calix[4]arenes **1a** and **2a** configurationally stable, thus preventing the "oxygen-through the annulus" rotation.[15] We then focused on optimising the enantioselective cyclisation reaction by screening a series of chiral gold(I) catalysts (Table 1; see the SI for full screening).

Initially, chiral phosphoramidite–gold complexes [$\mathbf{L_1}$AuCl] (bearing a 2-naphthyl group at the C3/C′3 positions) and [$\mathbf{L_2}$AuCl] (9-pyrenyl) were tested. While both gave excellent yields of **2a** (99% and 89%, respectively), the enantioselectivities were modest or low (*e.r.* = 74 : 26 and 57 : 43, respectively; entries 1 and 2). We next explored bidentate chiral ligands, such as $\mathbf{L_3}$ and $\mathbf{L_4}$, belonging to the BIPHEP family. [$\mathbf{L_3}(AuCl)_2$] afforded **2a** in an 89% yield but with poor enantiocontrol, while [$\mathbf{L_4}(AuCl)_2$] gave slightly improved enantioselectivity (*e.r.* = 72 : 28), though still unsatisfactory (entries 3 and 4). The

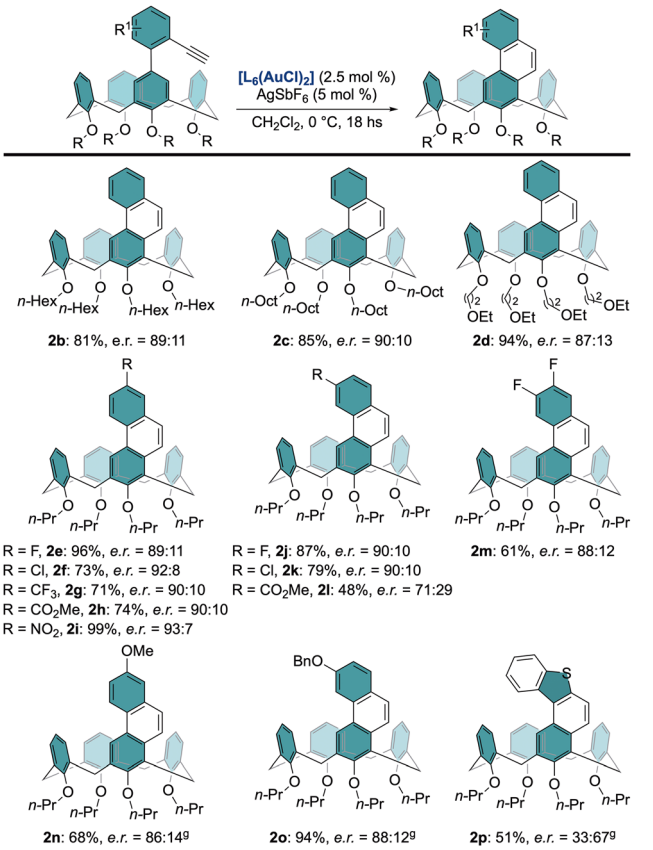

Scheme 2 Scope of the reaction. Reaction conditions: **1b–p** (0.065 mmol), [$\mathbf{L_6}(AuCl)_2$] (2.5 mol%), $AgSbF_6$ (5 mol%) in anhydrous CH_2Cl_2 (0.1 M) at 0 °C for 18 hours. Isolated yields are reported. [g] At room temperature.

(*R*)-DTBM-Segphos complex [$\mathbf{L_5}(AuCl)_2$] performed similarly to $\mathbf{L_4}$ (entry 5), whereas (*R*)-DM-Segphos [$\mathbf{L_6}(AuCl)_2$] delivered **2a** in a 91% yield and a promising *e.r.* of 86 : 14 (entry 6). With $\mathbf{L_6}$ as the most effective ligand, we examined the influence of the counterion. The use of $AgSbF_6$ resulted in a slight improvement in enantioselectivity (entry 7). Other counterions tested in the gold(I)-catalysed hydroarylation proved less effective (entries 8 and 9). In contrast, switching the solvent to toluene negatively affected the reaction, giving racemic **2a** in a 65% yield. Dichloromethane, on the other hand, improved both the yield and the enantiomeric ratio (99%, *e.r.* = 90 : 10), and was selected as the optimal reaction medium (entry 11). Finally, performing the reaction at 0 °C for 18 hours led to a satisfactory *e.r.* of 93 : 7 and a 95% yield (entry 12). With the optimized reaction conditions, we next evaluated the generality of the transformation by testing a series of functionalized calix[4]arenes **1b–p** (Scheme 2).

At the outset, modifications at the lower rim of the calix[4]arene core were examined. Tetrahexyl- and tetraoctyloxy-substituted calix[4]arenes **1b** and **1c** afforded the corresponding hydroarylated products **2b** and **2c** in high yields (81% and 85%) with enantiomeric ratios of 89 : 11 and 90 : 10, respectively. An even higher yield was obtained using the ethoxylated scaffold **1d**, which delivered **2d** in a 94% yield, albeit with a slightly lower enantioselectivity (*e.r.* = 87 : 13).

Keeping the tetrapropyl alkyl chain at the lower rim, we then introduced substituents with various electronic properties in the phenylacetylene ring. The reaction proved tolerant to a range of electron-withdrawing groups (F, Cl, CF_3, CO_2Me, NO_2) at the *meta*-position with respect to the alkyne moiety, affording the corresponding products **2e–i** in yields ranging from 71% to 99% and enantiomeric ratios of up to 93 : 7.

Similar results were obtained with halogens at the *para*-position: fluoro-, chloro- derivatives **2j** and **2k** were isolated in 87% and 79% yields, respectively, both with an *e.r.* of 90 : 10. In contrast, the methoxycarbonyl-substituted product **2l** showed lower reactivity and selectivity (48%, *e.r.* = 71 : 29). Likewise, difluoro-calix[4]arene **1m** was less reactive, giving **2m** in a 61% yield and an *e.r.* of 88 : 12. Electron-donating groups were also tolerated at various positions of the calix[4]arene scaffold. Hence, *meta*-OMe and *para*-OBn afforded the corresponding products **2n** and **2o** in moderate to excellent yields (68 and 94%, respectively). However, these reactions required higher temperatures (room temperature instead of 0 °C), and enantiocontrol was slightly reduced (*e.r.* = 86 : 14 and 88 : 12, respectively). Finally, thiophene-containing product **2p** could also be synthesized, albeit with modest yield (51%) and poor enantioselectivity. The structure and absolute configuration of the ICCs were further elucidated through X-ray single-crystal diffraction analysis of calix[4]arene **2f** and **2k**.

Four of the new ICCs were chosen for complete characterization of the (chiro-)optical properties, particularly **2a** (the reference compound), **2f** (*meta* chloride), **2h** (*meta* CO_2Et) and **2i** (*meta* nitro). Absorption, fluorescence and circular dichroism (CD) spectra were collected in two solvents of different polarity, hexane and dichloromethane (DCM). The main data in CH_2Cl_2 are reported in Fig. 1 (spectra in hexane in Fig. S1) and summarized in Table S1 (see the SI). All the compounds are characterized by strong absorption ($\varepsilon \sim 30\,000$–$60\,000$ L mol^{-1} cm^{-1}) in the UV. Compounds **2a**, **2f** and **2h** show weakly allowed transitions ($\varepsilon \sim 100$–1000 L mol^{-1} cm^{-1}) around 330–340 nm, likely of charge transfer (CT) nature. Since fluorescence emission always stems from the lowest-energy excited state, the observed Stokes shifts are very large (Fig. 1 and Table S1). For calixarene **2i**, the lowest-energy absorption band is quite intense and solvatochromic, moving from 345 nm in hexane to 360 in CH_2Cl_2, confirming the CT nature of the transition. Unfortunately, **2i** has no detectable emission in hexane, while in CH_2Cl_2 a red-shifted, broad emission band is recorded, associated with the same CT transition. In general, quantum yields are higher, and fluorescence lifetimes are longer in CH_2Cl_2 than in hexane (Table S1). All the compounds show positive CD peaks in the region of the main absorption bands in the visible range, while the sign changes for the band in the UV. **2i** also has a broad CD-active band at ~350 nm, associated with the CT transition, while for the other compounds these low-energy bands are extremely weak, as already observed in absorption. The dissymmetry factors ($g_{abs} = \Delta\varepsilon/\varepsilon$) are plotted in Fig. S2. The $|g_{abs}|$ are in general about 10^{-3}, indicating weak chiroptical activity, consistent with the small dimensions of the inherently chiral chromophore. The highest $|g_{abs}|$ are observed for **2f**, reaching values $> 2 \times 10^{-3}$.

Finally, we investigated the origin of the observed enantioselectivity by means of DFT calculations (see the SI for details). We located twelve transition states (TSs) for each enantiomeric product, for the gold-catalysed C–C bond formation (see relative energies and the optimized structures of selected TSs in Fig. 2). The TS associated with the lowest energy (**P_tilt_out_O2_C1**) leads to the formation of the experimentally observed major enantiomer *P*, while the lowest energy TS leading to the enantiomer *M* (**M_tilt_in_O2_C2**) is only 0.6 kcal mol^{-1} higher in energy. This energy difference would correspond to a 74 : 26 *e.r.* However, a few TSs are similar in energy, and would thus contribute to the product

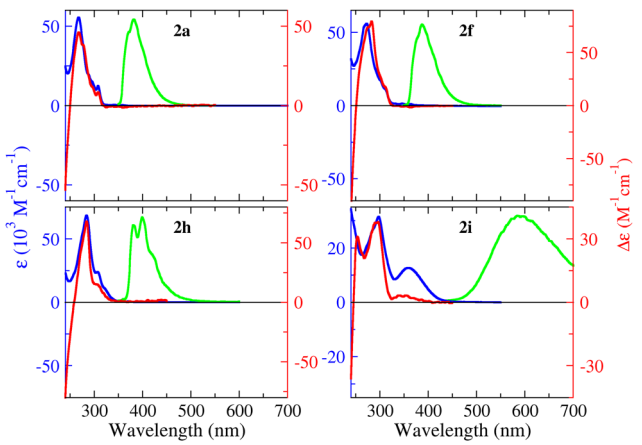

Fig. 1 Absorption (blue lines, left axes, molar extinction coefficient units), emission (green lines, arbitrary units) and CD spectra (red lines, right axes, $\Delta\varepsilon = \varepsilon_L - \varepsilon_R$) of compounds **2a**, **2f**, **2h** and **2i** in CH_2Cl_2.

				P	*M*
pinched	out	O1	C1	6.0	7.8
			C2	3.7	1.9
		O2	C1	7.4	5.6
			C2	12.1	2.3
tilted	out	O1	C1	7.8	5.5
			C2	7.3	9.8
		O2	C1	**0.0**	7.8
			C2	0.1	5.5
	in	O1	C1	9.6	4.7
			C2	1.4	4.7
		O2	C1	7.8	5.9
			C2	10.9	**0.6**
			Total %	83	17

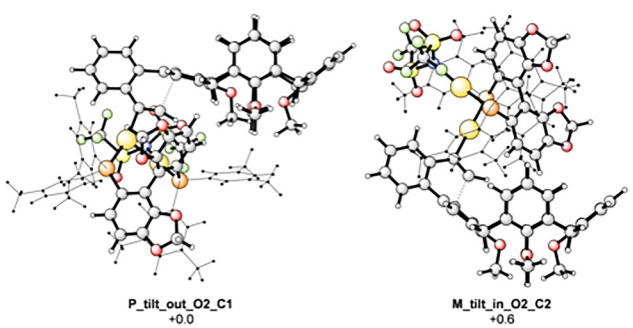

Fig. 2 Relative energies of the DFT-optimized transition states (top) and lowest energy transition states leading to the two enantiomers (bottom).

distribution. Boltzmann averaging all possible TS energies gives an 83 : 17 *e.r.*, in good agreement with the experimental results. Regarding the origin of the enantioselectivity, comparing the lowest energy TSs suggests that **P_tilt_out_O2_C1** is less sterically crowded than **M_tilt_in_O2_C2**. Moreover, the Au–Au interatomic distance is shorter in **P_tilt_out_O2_C1** than in **M_tilt_in_O2_C2** (3.13 *vs.* 3.28 Å), which could also contribute to the enantioselectivity of the reaction. In conclusion, we have developed the first enantioselective gold(I)-catalysed hydroarylation of alkynes for inherently chiral calix[4]arenes. Despite the intrinsic complexity of achieving high enantiocontrol in these sterically demanding alkynyl-functionalised macrocycles,[16] the method is general, operationally simple, and affords a broad range of ICCs in good yields and moderate to good enantioselectivities. Complementary computational studies rationalised the observed selectivities, while detailed chiroptical and photophysical analyses revealed structural and electronic properties that influence the optical behaviour of the final products. This catalytic method paves the way for the gold catalysed enantioselective synthesis of other calix[*n*]arene macrocycles.

Dr Elisa Brambilla is gratefully acknowledged. Mass spectrometry analyses were performed at the MS facility of the Unitech COSPECT (University of Milan). We acknowledge the CINECA award under the ISCRA initiative, for the availability of high performance computing resources and support. This work has benefited from the equipment and framework of the COMP-HUB and COMP-R Initiatives, funded by the ''Departments of Excellence'' program of the Italian Ministry for University and Research (MIUR, 2018-2022 and MUR, 2023-2027). This project was funded by the Italian MIUR (PRIN 20227Z3BL8).

Conflicts of interest

There are no conflicts to declare.

Data availability

The data supporting this article have been included as part of the supplementary Information (SI). See DOI: **https://doi.org/10.1039/d5cc04405g**.

CCDC 2476429 (**2f**) and 2476430 (**2k**) contain the supplementary crystallographic data for this paper.[17a,b]

Notes and references

1 L. Ackermann, T. B. Gunnoe and L. G. Habgood. *Catalytic Hydroarylation of Carbon-Carbon Multiple Bonds*, Wiley-VCH, Weinheim Germany, 2018.
2 (*a*) T. Ghosh, J. Chatterjee and S. Bhakta, *Org. Biomol. Chem.*, 2022, **20**, 7151; (*b*) G. Zuccarello, I. Escofet, U. Caniparoli and A. M. Echavarren, *ChemPlusChem*, 2021, **86**, 1283; (*c*) R. Dorel and A. M. Echavarren, *Chem. Rev.*, 2015, **115**, 9028.
3 (*a*) Y.-B. Wang, W. Liu, T. Li, Y. Lu, Y.-T. Yu, H.-T. Liu, M. Liu, P. Li, P.-C. Qian, H. Tang, J. Guan, L.-W. Ye and L. Li, *J. Am. Chem. Soc.*, 2024, **146**(49), 33804; (*b*) Q. Gaignard-Gaillard, X. Han, A. Alix, C. Bour, R. Guillot, V. Gandon and A. Voituriez, *Adv. Synth. Catal.*, 2022, **364**, 4415; (*c*) J. Zhang, M. Simon, C. Golz and M. Alcarazo, *Angew. Chem., Int. Ed.*, 2020, **59**, 5647; (*d*) M. Satho, Y. Shibata, Y. Kimura and K. Tanaka, *Eur. J. Org. Chem.*, 2016, 4465.
4 (*a*) P.-C. Zhang, Y.-L. Li, J. He, H.-H. Wu, Z. Li and J. Zhang, *Nat. Commun.*, 2021, **12**, 4609; (*b*) A. Urbano, G. Hernández-Torres, A. M. del Hoyo, A. Martínez-Carrióna and M. C. Carreño, *Chem. Commun.*, 2016, **52**, 6419.
5 (*a*) L. D. M. Nicholls, M. Marx, T. Hartung, E. González-Fernández, C. Golz and M. Alcarazo, *ACS Catal.*, 2018, **8**, 6079; (*b*) E. González-Fernández, L. D. M. Nicholls, L. D. Schaaf, C. Farès, C. W. Lehmann and M. Alcarazo, *J. Am. Chem. Soc.*, 2017, **139**, 1428.
6 M. Tang and X. Yang, *Eur. J. Org. Chem.*, 2023, e202300738.
7 (*a*) V. Böhmer, D. Kraft and M. Tabatabai, *J. Inclusion Phenom. Mol. Recognit. Chem.*, 1994, **19**, 17; (*b*) A. Dalla Cort, L. Mandolini, C. Pasquini and L. Schiaffino, *New J. Chem.*, 2004, **28**, 1198.
8 (*a*) W. Qin and G. Cera, *Chem. Rec.*, 2025, **25**, e202400237; (*b*) P. Lhoták, *Org. Biomol. Chem.*, 2022, **20**, 7377–7390.
9 (*a*) S. Tong, J.-T. Li, D.-D. Liang, Y.-E. Zhang, Q.-Y. Feng, X. Zhang, J. Zhu and M.-X. Wang, *J. Am. Chem. Soc.*, 2020, **142**, 14432; (*b*) X. Zhang, S. Tong, J. Zhu and M.-X. Wang, *Chem. Sci.*, 2023, **14**, 827; (*c*) Y.-Z. Zhang, M.-M. Xu, X.-G. Si, J.-L. Hou and Q. Cai, *J. Am. Chem. Soc.*, 2022, **144**, 22858; (*d*) T. Li, Y. Zhang, C. Du, D. Yang, M.-P. Song and J.-L. Niu, *Nat. Commun.*, 2024, **15**, 7673; (*e*) L. Zhang, C. Yang, X. Wang, T. Yang, D. Yang, Y. Dou and J.-L. Niu, *Green Chem.*, 2024, **26**, 10232; (*f*) P.-F. Qian, G. Zhou, J.-H. Hu, B.-J. Wang, A.-L. Jiang, T. Zhou, W.-K. Yuan, Q.-J. Yao, J.-H. Chen, K.-X. Kong and B.-F. Shi, *Angew. Chem., Int. Ed.*, 2024, **63**, e202412459; (*g*) Y.-K. Jiang, Y.-L. Tian, J. Feng, H. Zhang, L. Wang, W.-A. Yang, X.-D. Xu and R.-R. Liu, *Angew. Chem., Int. Ed.*, 2024, **63**, e202407752; (*h*) S. Yu, M. Yuan, W. Xie, Z. Ye, T. Qin, N. Yu and X. Yang, *Angew. Chem., Int. Ed.*, 2024, **63**, e202410628; (*i*) X.-Y. Zhang, D. Zhu, R.-F. Cao, Y.-X. Huo, T.-M. Ding and Z.-M. Chen, *Nat. Commun.*, 2024, **15**, 9929; (*j*) V. Dočekal, L. Lóška, A. Kurčina, I. Císařová and J. Veselý, *Nat. Commun.*, 2025, **16**, 4443.
10 (*a*) G. E. Arnott, *Chem. – Eur. J.*, 2018, **24**, 1744; (*b*) S.-Y. Li, Y.-W. Xu, J.-M. Liu and C.-Y. Su, *Int. J. Mol. Sci.*, 2011, **12**, 429; (*c*) A. Szumna, *Chem. Soc. Rev.*, 2010, **39**, 4274.
11 Q. He, G. I. Vargas-Zúñiga, S. H. Kim, S. K. Kim and J. L. Sessler, *Chem. Rev.*, 2019, **119**, 9753.
12 (*a*) G. Sachdeva, D. Vaya, C. M. Srivastava, A. Kumar, V. Rawat, M. Singh, M. Verma, P. Rawat and G. K. Rao, *Coord. Chem. Rev.*, 2022, **472**, 214791; (*b*) O. Santoro and C. Redshaw, *Coord. Chem. Rev.*, 2021, **448**, 214173.
13 (*a*) G. Giovanardi, S. Cattani, D. Balestri, A. Secchi and G. Cera, *J. Org. Chem.*, 2024, **89**, 8486; (*b*) G. Giovanardi, G. Scarica, V. Pirovano, A. Secchi and G. Cera, *Org. Biomol. Chem.*, 2023, **21**, 4072; (*c*) G. Cera, G. Giovanardi, A. Secchi and A. Arduini, *Chem. – Eur. J.*, 2021, **27**, 10261.
14 K. Iwamoto, K. Araki and S. Shinkai, *J. Org. Chem.*, 1991, **56**, 4955.
15 S. Shinkai, T. Arimura, H. Kawabata, H. Murakami and K. Iwamoto, *J. Chem. Soc., Perkin Trans. 1*, 1991, 2429.
16 For examples using tailored-designed ligands, see: (*a*) G. Zuccarello, J. G. Mayans, I. Escofet, D. Scharnagel, M. S. Kirillova, A. H. Pérez-Jimeno, P. Calleja, J. R. Boothe and A. M. Echavarren, *J. Am. Chem. Soc.*, 2019, **141**, 11858; (*b*) U. Caniparoli, I. Escofet and A. M. Echavarren, *ACS Catal.*, 2022, **12**, 3317; (*c*) A. Franchino, À. Martí and A. M. Echavarren, *J. Am. Chem. Soc.*, 2022, **144**, 3497; (*d*) I. Martín-Torres, G. Ogalla, J.-M. Yang, A. Rinaldi and A. M. Echavarren, *Angew. Chem., Int. Ed.*, 2021, **60**, 9339; (*e*) G. Zuccarello, L. J. Nannini, A. Arroyo-Bondía, N. Fincias, I. Arranz, A. H. Pérez-Jimeno, M. Peeters, I. Martín-Torres, A. Sadurní, V. García-Vázquez, Y. Wang, M. S. Kirillova, M. Montesinos-Magraner, U. Caniparoli, G. D. Núñez., F. Maseras, M. Besora, I. Escofet and A. M. Echavarren, *JACS Au*, 2023, **3**, 1742.
17 (*a*) M. Goudarzi, A. Alagiyawanna, A. Serafino, S. Rizzato, F. Bertocchi, F. Terenziani, S. Santoro, W. Qin, G. Cera and V. Pirovano, CCDC 2476429: Experimental Crystal Structure Determination, 2025, DOI: **10.5517/ccdc.csd.cc2p3xtk**; (*b*) M. Goudarzi, A. Alagiyawanna, A. Serafino, S. Rizzato, F. Bertocchi, F. Terenziani, S. Santoro, W. Qin, G. Cera and V. Pirovano, CCDC 2476430: Experimental Crystal Structure Determination, 2025, DOI: **10.5517/ccdc.csd.cc2p3xvl**.